

Effect of oxygen isotope substitution on charge ordering and magnetic and transport properties in $\text{Pr}_{0.5}\text{Ca}_{0.5}\text{MnO}_3$ doped by chromium and ruthenium

N. A. Babushkina,¹ A. N. Taldenkov,¹ A. V. Inyushkin,¹ A. Maignan,² D. I. Khomskii,³ and K. I. Kugel⁴

¹Russian Research Center “Kurchatov Institute,” Kurchatov Square 1, 123182 Moscow, Russia

²Laboratoire CRISMAT, ENSICAEN, 6 Boulevard du Maréchal Juin, 14050 Caen Cedex 4, France

³Physikalisches Institut, Universität zu Köln, Zùlpicher Strasse 77, 50937 Köln, Germany

⁴Institute for Theoretical and Applied Electrodynamics, Russian Academy of Sciences, Izhorskaya Str. 13, Moscow 125412, Russia

(Received 18 September 2008; revised manuscript received 16 November 2008; published 30 December 2008)

The effect of the $^{16}\text{O} \rightarrow ^{18}\text{O}$ isotope substitution on the properties of the $\text{Pr}_{0.5}\text{Ca}_{0.5}\text{MnO}_3$ manganites doped by Cr and Ru is studied. In these compounds, chromium and ruthenium favor (i) the suppression of a charge-ordered state and (ii) the formation of a ferromagnetic metallic clusters. The $^{16}\text{O} \rightarrow ^{18}\text{O}$ isotope substitution leads to an increase in the charge-ordering transition temperature (T_{CO}) and to the lowering of ferromagnetic transition temperature (T_{FM}) accompanied by a decrease in the content of ferromagnetic phase. The difference in the properties of the Cr- and Ru-doped compounds is analyzed.

DOI: 10.1103/PhysRevB.78.214432

PACS number(s): 75.47.Lx, 75.30.Kz

I. INTRODUCTION

Rare-earth manganites $R_{1-y}A_y\text{MnO}_3$ (R =rare-earth metal; A =Ca, Sr, Ba) exhibit a characteristic tendency to phase separation that leads to the formation of an inhomogeneous ground state, in which a ferromagnetic (FM) metallic phase coexists with an antiferromagnetic (AFM) insulating phase.¹⁻³ This tendency is most clearly pronounced in manganites close to half doping ($y=0.5$), where a charge-ordered (CO) state with the CE-type magnetic structure appears and the phase separation takes place as a result of the competition between the charge-ordered and orbitally ordered (CO-OO) AFM and FM phases.⁴⁻⁸ The charge ordering leads to a checkerboard arrangement of Mn^{3+} and Mn^{4+} ions in the crystal lattice, whereby the CE-type magnetic structure is characterized by arrays of oppositely oriented FM zigzag spin chains of manganese ions lying within parallel AFM-ordered planes.⁶

The half-doped manganite $\text{Pr}_{0.5}\text{Ca}_{0.5}\text{MnO}_3$ has received much attention due to its unusual properties.⁷⁻⁹ This manganite is characterized by different temperatures of the charge and spin ordering: a charge-ordered phase appears at $T_{\text{CO}}=250$ K, whereas the AFM spin-ordered state of the CE type arises at $T_N < 165$ K.^{7,8} A strong magnetic field (10–30 T) is necessary to “melt” the charge-ordered phase and create an FM phase in $\text{Pr}_{0.5}\text{Ca}_{0.5}\text{MnO}_3$.¹⁰

It was found that the replacement of manganese ions in $\text{Pr}_{0.5}\text{Ca}_{0.5}\text{MnO}_3$ by other transition-metal ions (Cr, Ru, Ni, and Co) also leads to the breakdown of a charge-ordered state and the formation of FM order.¹¹⁻¹⁴ For example, an admixture of chromium as small as 2% is sufficient to induce the insulator-metal transition even at zero magnetic field. It was also demonstrated¹⁵ that $\text{Pr}_{0.5}\text{Ca}_{0.5}\text{Mn}_{1-x}\text{Cr}_x\text{O}_3$ can be considered as a system with phase separation, in which charge-ordered AFM regions coexist with FM regions. As the doping level x is increased, the fraction of the FM phase grows up to 90% at $x=0.05$.¹⁶

It turned out that not all transition-metal impurities destroy in the same manner the CO-OO state in half-doped $\text{Pr}_{0.5}\text{Ca}_{0.5}\text{Mn}_{1-x}\text{M}_x\text{O}_3$ manganites. Indeed, in

$\text{Pr}_{0.5}\text{Ca}_{0.5}\text{Mn}_{1-x}\text{M}_x\text{O}_3$ the coupling of Cr^{+3} ions with Mn^{+3} and Mn^{+4} in MnO_6 octahedra differs from that for Ru^{+4} or Ru^{+5} ion. The mechanisms underlying the destruction of zigzag spin chains in the CE structure of $\text{Pr}_{0.5}\text{Ca}_{0.5}\text{Mn}_{1-x}\text{M}_x\text{O}_3$ are not the same for these dopants. As a result the Ru-doped manganites show stronger ferromagnetic interactions and higher ferromagnetic transition point T_{FM} .^{17,18} This is caused both by different valence states (Cr^{+3} vs Ru^{+4} or even Ru^{+5}) and by different filling of electronic energy levels ($t_{2g}^3 e_g^0$ in Cr^{+3} and Ru^{+5} , $t_{2g}^3 e_g^1$ in Ru^{+4} vs $t_{2g}^3 e_g^1$ in Mn^{3+} , and $t_{2g}^3 e_g^0$ in Mn^{4+}). As discussed in Ref. 17, this leads to the formation of somewhat different ferromagnetic “metallic” clusters around Cr and Ru dopants (larger clusters around Cr and smaller clusters with “stronger” ferromagnetism around Ru).

The oxygen isotope substitution has been previously used as a unique tool for studying various features of phase separation in manganites.^{19,20} In particular, it was established that the isotope substitution produces an unusually strong effect on the transport and magnetic properties of $(\text{La}_{1-x}\text{Pr}_x)_{0.7}\text{Ca}_{0.3}\text{MnO}_3$ in the region of crossover between the FM- and AFM-ordered states.¹⁹ The substitution of ^{16}O by ^{18}O induced a transition between the FM metallic and the charge-ordered AFM insulating phases.

The recent studies demonstrated that a pronounced isotope effect due to the $^{16}\text{O} \rightarrow ^{18}\text{O}$ substitution could be expected in the vicinity of a crossover between different types of ground states (in particular, between CO-OO and FM). Earlier, such isotope effect was found in the systems with the doping level being far from the optimum value for charge ordering at $x=0.5$. This leads to a lower stability of the CO-OO phase. It was already mentioned above that the CO-OO state is also destabilized by Cr and Ru dopants, whereas the charge-carrier density remains close to that of the half-doped case ($x=0.5$). Thus, it is interesting to find out whether the $^{16}\text{O} \rightarrow ^{18}\text{O}$ isotope substitution leads to strong effects in such a situation as well. This should provide a better insight into the nature of isotope effect. The preliminary study of isotope effect in chromium-doped manganites²¹ clearly demonstrated that magnetic and electric properties are strongly dependent on average oxygen mass. Following

the findings in Ref. 21, we would also like to know whether an isotope effect is sensitive to the specific type of impurity (Cr or Ru), which differs in the mechanisms of suppression of the CO-OO state.

In this paper, we present an experimental study of the isotope effect in $\text{Pr}_{0.5}\text{Ca}_{0.5}\text{MnO}_3$ compound doped by Cr and Ru. The measurements of magnetization, ac magnetic susceptibility, and magnetoresistance were performed for the $\text{Pr}_{0.5}\text{Ca}_{0.5}(\text{Mn}_{1-x}\text{Cr}_x)^{16-18}\text{O}_3$ system at $x=0, 0.02, \text{ and } 0.05$ (the samples referred to as Cr0, Cr2, and Cr5, respectively) and for $\text{Pr}_{0.5}\text{Ca}_{0.5}(\text{Mn}_{1-x}\text{Ru}_x)^{16-18}\text{O}_3$ with $x=0.01, 0.02, \text{ and } 0.05$ (the samples referred to as Ru1, Ru2, and Ru5, respectively).

II. EXPERIMENTAL

The ceramic samples of $\text{Pr}_{0.5}\text{Ca}_{0.5}\text{MnO}_3$ manganites doped by Cr and Ru were prepared in the form of pellets using the solid-phase synthesis technique (see the details in Ref. 11). A stoichiometric mixture of initial oxides (CaCO_3 , Cr_2O_3 , Mn_2O_3 , and Pr_6O_{11}) was annealed in air at 950°C for 12 h. After that the powder was pressed into pellets and sintered at 1200°C . A single-phase composition of samples was checked by x-ray diffraction. The $^{16}\text{O} \rightarrow ^{18}\text{O}$ oxygen isotope substitution was carried out by heating at 950°C and a gas pressure of 1 bar for 200 h. Two samples of a rectangular shape prepared from the same piece of the initial material were simultaneously annealed, one in $^{16}\text{O}_2$ and the other in $^{18}\text{O}_2$ (93% of $^{18}\text{O}_2$). The final enrichment of the samples with ^{18}O was 92%, as determined from the weight change. The enrichment process was described in detail elsewhere.¹⁹ The similarity of the oxygen isotope composition in the sample to that in the gas medium indicated that a thermodynamic equilibrium was achieved in the course of annealing and, hence, the difference in the diffusion rates of oxygen isotopes did not significantly affect the results of investigation. It should be also noted that the mass of a sample annealed in $^{16}\text{O}_2$ remained unchanged (to within the experimental error) in the course of the prolonged heat treatment. From this, we conclude that the annealing procedure does not change the stoichiometric oxygen content in the compound under study. Estimates from above, based on the experimental error of sample weighing, show that the oxygen content remains constant to within 0.01.

The electrical resistance $R(T)$ of the samples was measured using the four-probe technique at temperatures ranging from 5 to 330 K and magnetic fields up to 4 T [a two-probe method was used in the case $R(T) > 1\ \text{G}\Omega$]. Magnetic field was directed parallel to the transport current in the samples. The differential magnetic susceptibility $\chi(T)$ was measured in an ac magnetic field with a frequency of 667 Hz and amplitude of 5 Oe. The magnetization measurements were performed by a Hall-probe technique. The GaAs planar-type commercial Hall sensors THS118 were used as sensitive elements (for details see Ref. 22). Three preselected sensors with similar characteristics were employed to measure the distribution of magnetic field in the experimental cell. Two sensors were used to determine z component of induction B in the vicinity of the flat ends of the samples with natural and

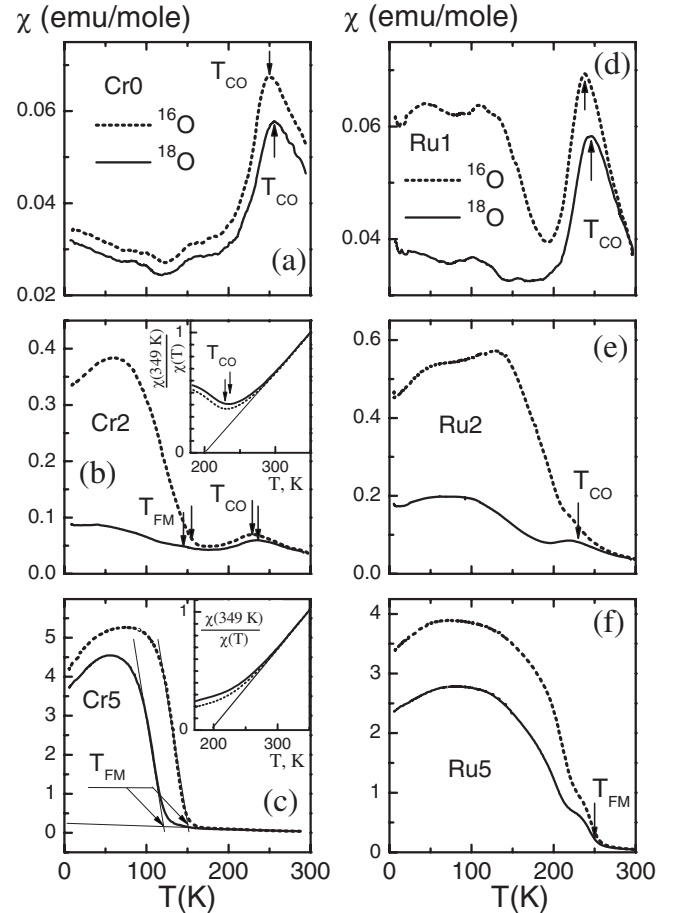


FIG. 1. Temperature dependences of the real part of magnetic susceptibility $\chi(T)$ of the manganite $\text{Pr}_{0.5}\text{Ca}_{0.5}\text{Mn}^{16-18}\text{O}_3$ with Cr and Ru impurities measured on cooling (dashed line corresponds to ^{16}O and solid line to ^{18}O). Arrows indicate T_{CO} [panels (a), (b), (d), and (e)] and T_{FM} [panels (c) and (f)]; straight lines in panel (c) illustrate the manner for determination of the T_{FM} . The insets of panels (b) and (c) show the reciprocal susceptibility $\chi(349\ \text{K})/\chi(T)$ curves for Cr2 and Cr5 samples, respectively, in the vicinity of T_{CO} in an extended scale.

heavy oxygen. The third one measured the external applied magnetic field H and was used for taking into account the temperature and field dependences of the sensitivity of sensors. The data for both samples and applied magnetic field were obtained simultaneously. The effective magnetization $M=B-H$ was calculated (in millitesla units) for a local area of the magnetic material at temperatures of 5–300 K in magnetic fields of 0.05–4 T. The $\chi(T)$ and $R(T)$ data for chromium-doped samples were adopted from Ref. 21.

The charge-ordering temperature (T_{CO}) was determined from the maximum of $\chi(T)$ [Fig. 1(a)]. According to Ref. 23, this maximum coincides with the onset of other structural features, which are characteristic of charge ordering. The temperature T_{FM} of the onset of FM ordering was determined by extrapolating the $\chi(T)$ or $M(H)$ plot to the background [Fig. 1(c)]. The temperature T_{MI} of the metal-insulator transition was determined from the position of maximum on the $R(T)$ curve [Fig. 3(c)]. All these transition temperatures were determined using the curves measured on cooling.

III. RESULTS

A. ac susceptibility and magnetization

Figure 1 shows the temperature dependence of the ac magnetic susceptibility, $\chi(T)$, for the samples with different isotope compositions. In undoped $\text{Pr}_{0.5}\text{Ca}_{0.5}\text{MnO}_3$ with the light oxygen isotope (Cr0 sample), the charge-ordered state appears at $T_{\text{CO}}=250\pm 2$ K, which decreases down to 229 ± 2 K in the samples (Cr2) doped by 2% of chromium. Charge-ordered state is well developed in Cr2 samples; this is clearly seen on reciprocal susceptibility [inset of Fig. 1(b)]. The high-temperature susceptibility obeys the Curie-Weiss law $\chi^{-1}\propto(T-T_C)$ with positive value of Curie temperature $T_C\approx 200$ K. The dip at the onset of charge-ordering transition reflects the change of magnetic interaction from FM to AFM as the temperature decreases.

The characteristic peak in $\chi(T)$ corresponding to the formation a charge-ordered state is strongly suppressed in the samples containing 5% of chromium. Nevertheless, the deviation from Curie-Weiss law is clearly seen [inset of Fig. 1(c)]. There is no dip like in Cr2 samples (inset of Fig. 1(b)), but change in slope of $\chi^{-1}(T)$ demonstrates the competition between FM and AFM interactions and in Cr5 samples and the effective value of T_C in the Curie-Weiss law decreases as temperature goes down. It indicates that the charge order may exist in Cr5 samples, but possibly it is a short-range order.

The Cr-doped compounds demonstrate signatures of the FM state formation at temperature below $T_{\text{FM}}=153\pm 7$ K (Cr2) and $T_{\text{FM}}=150\pm 2$ K (Cr5). One can see that low-temperature ac susceptibility in Cr2 samples is about 1 order of magnitude less than that in Cr5. As the low-temperature ferromagnetic moment in Cr5 samples is practically saturated and FM fraction is higher than 90%,¹⁶ it is evident that FM phase in Cr2 sample only partially occupies the volume and this compound can be considered as a system exhibiting a phase separation with the coexistence of charge-ordered and FM regions.

The $^{16}\text{O}\rightarrow^{18}\text{O}$ oxygen isotope substitution modifies the magnetic phase diagram of the $\text{Pr}_{0.5}\text{Ca}_{0.5}\text{Mn}_{1-x}\text{Cr}_x\text{O}_3$ system. In Cr0 and Cr2 samples, the $^{16}\text{O}\rightarrow^{18}\text{O}$ isotope substitution leads to increase in T_{CO} by 4 and 7 K, respectively [Figs. 1(a) and 1(b)]. In Cr2 and Cr5 samples, this substitution reduces the values of T_{FM} by 13 and 28 K [Figs. 1(b) and 1(c)]. The maximum effect of the oxygen isotope substitution on the phase-separation process is observed in Cr2. This sample is characterized by a small content of the FM phase and broad transition. It is why the accurate determination of T_{FM} in the ^{18}O -rich Cr2 sample is difficult. The estimate of $T_{\text{FM}}=140\pm 15$ K in this sample is very rough and only indicates the possible region of temperatures corresponding to the onset of the FM-order formation. It was impossible to reveal the isotope substitution effect on the magnetic susceptibility and parameters of Curie-Weiss constant at room temperatures as it was done in Ref. 24 because of a large error of determination of the absolute value of $\chi(T)$ at temperatures approaching 300 K.

The behavior of $\chi(T)$ at different doping levels and different isotope substitution for $\text{Pr}_{0.5}\text{Ca}_{0.5}\text{Mn}_{1-x}\text{M}_x\text{O}_3$ with M

=Ru is nearly the same as for manganites with Cr. The amount of CO phase decreases and the fraction of a FM phase increases with increase in Ru concentration. The $^{16}\text{O}\rightarrow^{18}\text{O}$ isotope substitution leads to the shift of T_{CO} toward higher temperatures and to the decrease in T_{FM} [Figs. 1(d) and 1(e)]. The values of T_{CO} in Ru1 samples are 237 K for the samples with ^{16}O , and this value increases by 7 K at substitution of ^{16}O by ^{18}O [Fig. 1(d)]. For Ru2 samples, the percentage of the charge-ordered phase steeply decreases, and the FM phase appears, which mainly determines the value of $\chi(T)$. The charge-ordered phase manifests itself only slightly in the temperature dependence of $\chi(T)$ of sample with ^{16}O . On the other hand, this phase is clearly distinguishable in $\chi(T)$ curves for samples with ^{18}O [Fig. 1(e)].

There are some specific features determined by the aforementioned difference in interactions of Cr and Ru ions with Mn. As mentioned above, embedded Ru ions lead to a stronger FM interaction in the Ru-doped compound and hence to a higher temperature of the FM transition. The temperatures of a transition to a FM phase are close to the temperatures of a transition to the CO phase just in Ru2 samples with ^{16}O . Both phases coexist at the same temperature range and it is difficult to distinguish the onset of the FM and CO transitions. The estimates for the isotope shift are very rough: $\Delta T_{\text{CO}}\approx 6$ K and $\Delta T_{\text{FM}}\approx 30$ K for Ru2 samples.

For Ru5 samples the fraction of the FM phase grows significantly and CO phase is observed on this ferromagnetic background. The CO and FM phases compete with each other. For these reason, the experimental errors in determination of T_{CO} and T_{FM} are large and we may give only rough estimates: $T_{\text{CO}}\approx 240$ K and $T_{\text{FM}}\approx 250$ K. However, one clearly sees that oxygen isotope shift goes to zero in Ru5 samples.

Note that in Cr- and Ru-doped samples enriched by ^{18}O the maximum value of the magnetic susceptibility is smaller in comparison with the samples with ^{16}O . This signals the decrease in the fraction of a FM phase in the phase-separated regime. The maximum effect of the oxygen isotope substitution on the phase separation was observed for Cr2 and Ru2 samples.

The measurements of magnetization at different values of applied dc magnetic field were performed to determine more reliably the value of T_{FM} . The onset of FM ordering (T_{FM}) in Cr5 and Ru5 was determined by extrapolating the $M(T)$ to background. The values of T_{FM} determined in such a way are more accurate than those obtained based from ac magnetic susceptibility such as, in particular, for Ru5 samples. The temperature dependence of dc magnetization of Cr5 and Ru5 samples is shown in Fig. 2.

The well-defined FM transitions were observed. The $^{16}\text{O}\rightarrow^{18}\text{O}$ isotope substitution leads to the lowering of saturation value of M in both compounds and substantially decreases the onset of FM transition ($\Delta T_{\text{FM}}\approx 25$ K) in Cr5 samples. Magnetic field in its turn stabilizes FM ordering in the Cr5 samples at higher temperatures and leads to an increase in T_{FM} . The isotope shift of T_{FM} appears to be nearly independent of magnetic field in Cr5 samples. As for Ru5 samples, they demonstrate less sensitivity to magnetic field and the absence of isotope shift of T_{FM} within an experimental error in all applied fields.

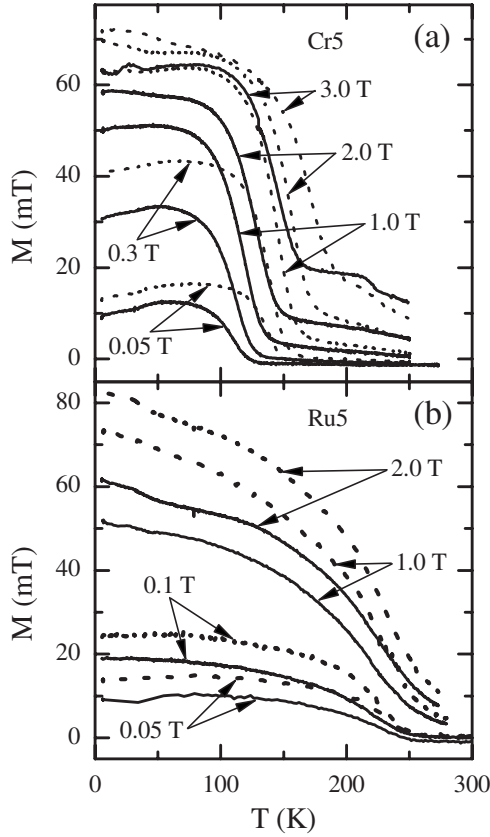


FIG. 2. Temperature dependences of magnetization $M(T)$ of $\text{Pr}_{0.5}\text{Ca}_{0.5}\text{Mn}^{16-18}\text{O}_3$ manganite doped by 5 at. % of (a) Cr and (b) Ru measured on cooling at different values of applied dc magnetic field (dashed lines correspond to ^{16}O and solid lines to ^{18}O).

B. Electrical resistance and magnetoresistance

In Fig. 3 the temperature dependence of the electrical resistance $R(T)$ for all samples measured at various applied magnetic fields is shown. These results confirm the validity of the data obtained from the magnetic-susceptibility measurements. The samples free of the FM phase (i.e., Cr0 and Ru1) exhibit a semiconductor behavior in the fields $H < 4$ T [Figs. 3(a) and 3(d)]. Both charge-ordered and FM phases coexist in Cr2 and Ru2 [Figs. 3(b) and 3(e)], and the content of the FM metal phase can be sufficient for the formation of an infinite conducting cluster. A large value of residual resistance and a low temperature of the metal-insulator transition ($T_{\text{MI}}=49$ K) (compared to $T_{\text{FM}}=153$ K) are indicative of a relatively small volume fraction of the FM metallic phase in Cr2 [Fig. 3(b)]. The application of a magnetic field leads to a decrease in the resistivity by several orders of magnitude [colossal magnetoresistance (CMR) effect], which is a signature of an increase in the content of the conducting FM phase. For the ^{18}O -rich Cr2 sample the FM phase content is smaller than that in ^{16}O -Cr2 and the $R(T)$ curve has a semiconductor character in magnetic fields below 3.7 T.

In Ru2 samples with ^{16}O and ^{18}O isotopes, the charge-ordered and ferromagnetic phases coexist [Fig. 3(e)], but the fraction of FM phase is not sufficient to form an infinite percolation cluster. In these Ru2 samples, the conductivity is

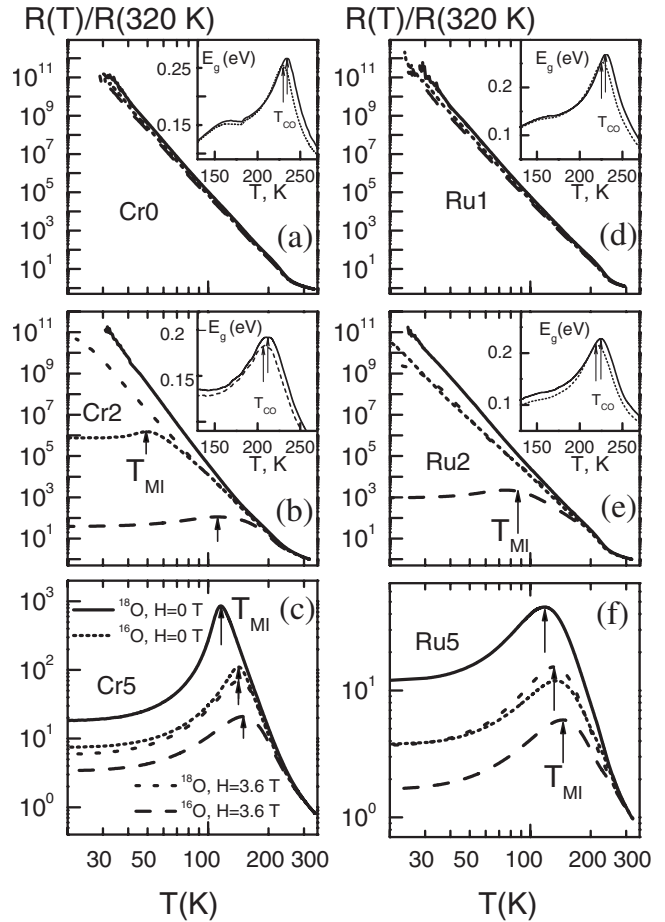


FIG. 3. Temperature dependences of the reduced resistance of the manganite $\text{Pr}_{0.5}\text{Ca}_{0.5}\text{Mn}^{16-18}\text{O}_3$ with Cr and Ru impurities with different isotope compositions measured at various magnetic fields on cooling (solid lines correspond to $^{18}\text{O}, H=0$ T, dotted lines to $^{16}\text{O}, H=0$ T, short dashed line to $^{18}\text{O}, H=3.6$ T, and dashed line to $^{16}\text{O}, H=3.6$ T). Arrows indicate the temperatures of the metal-insulator transition. The insets show temperature dependences of activation energy E_g at zero field. The arrows in the insets indicate the maximum of $E_g(T)$.

of semiconductor type in zero magnetic field. The applied magnetic field gives rise to an increase in the fraction of conducting FM phase leading eventually to the metal-insulator transition for Ru2 sample with ^{16}O . The metal-insulator transition temperature $T_{\text{MI}} \approx 50$ K is lower than $T_{\text{FM}} \approx 200$ K. It gives an indication of a slight growth of the volume concentration of FM phase at applied magnetic field $H=4$ T. Ru2 sample with ^{18}O has the semiconductor-type $R(T)$ at fields below 3.7 T, implying that the fraction of FM phase here is lower than in Ru2 sample with ^{16}O . Thus, the $^{16}\text{O} \rightarrow ^{18}\text{O}$ isotope substitution in Cr2 and Ru2 leads to a metal-insulator transition, which is analogous to a transition observed previously in $(\text{La}_{0.25}\text{Pr}_{0.75})_{0.7}\text{Ca}_{0.3}\text{MnO}_3$.¹⁹

The logarithmic derivative of Arrhenius plot gives the activation energy $E_g \propto \partial \ln(R) / \partial (1/T)$, which is a characteristic parameter of the semiconducting state. The insets of Figs. 3(a), 3(b), 3(d), and 3(e) show the temperature dependences of the E_g for both isotopes. The maximum of $E_g(T)$ corresponds to the point of maximal rate of the lattice parameters

change under charge ordering and it is positioned by about 20 K below the T_{CO} determined from the ac susceptibility.²³ The negative isotope shift of 5–6 K is clearly seen for all samples. Moreover, at $T > T_{CO}$, the value of E_g is systematically higher for samples with ^{18}O , suggesting the existence of the sizable isotope effect even at high temperatures.

The heavily doped Cr5 and Ru5 samples behave as ferromagnetic metals at low temperatures and as semiconductors at $T > T_{FM}$ [Figs. 3(c) and 3(f)]. The effect of the isotope substitution manifests itself by a decrease in T_{MI} and rise of the residual resistance with increasing of the oxygen mass. However, at this dopant concentration even the ^{18}O sample remains a “bad” metal despite of smaller metallic phase fraction. Note that the metal-insulator transition in Cr5 samples takes place when the magnetic susceptibility attains 20%–25% of the maximum value for the FM-saturated state [Figs. 1(c) and 2(a)]. This fact can be interpreted as an evidence for a bulk percolation transition taking place at a volume fraction of the FM metallic phase above 20%. The Ru5 samples demonstrate more complicated behavior. They turn out to be metallic ferromagnets at temperatures by approximately 100 K below the onset of the FM transition [Fig. 3(f)] and have nearly the same T_{MI} as Cr5 samples. This fact shows that the process of nucleation and growth of FM fraction below T_{FM} is much steeper in Cr5 compounds. In contrast, the $R(T_{MI})/R(320\text{ K})$ ratio in Ru5 sample is less by a factor of 20 than that in Cr5. It confirms that conductivity in Ru5 samples at $T_{MI} < T < T_{FM}$ is of a mixed type: conducting FM clusters are immersed into the insulating matrix. The existence of large magnetoresistance far above T_{MI} in Ru5 samples [Fig. 3(f)] also confirms this suggestion, whereas in Cr5 samples CMR effect develops in the close vicinity of T_{MI} [Fig. 3(c)]. Note that T_{MI} in our Ru5 samples is lower than that observed earlier in Ref. 16. This difference in transport properties could arise from the smaller grain size and higher porosity of our ceramics due to lower sintering temperature (1200 °C).

The resulting H - T diagram summarizes the effect of magnetic field and isotope substitution on Cr5 and Ru5 compounds (Fig. 4). We see that both in Cr5 and Ru5, the metal-insulator transition occurs at temperatures substantially below T_{FM} . This suggests an appreciable inhomogeneity of the sample at $T < T_{FM}$ (a mixture of a FM metal and an insulator). However, the nature of the insulating phase in Cr5 is not quite clear since the x-ray diffraction data did not provide any evidence of the long-range charge ordering.¹⁶ At the same work authors report that T_{MI} in Ru5 samples may be close to T_{FM} . This disagreement with present work shows that our samples may have additional structural details such as insulating boundaries and disorder, which block the conductivity and diminish T_{MI} .

The investigation of the spin-dependent transport in non-metallic and nonferromagnetic media is an effective method for studying the details of magnetic background in manganites. It is well known²⁵ that on nonferromagnetic side of the phase diagram the conductivity in a magnetic field is controlled by local magnetization,

$$\rho = \rho_0 \exp[-(E_g - Wm^2)/k_B T], \quad (1)$$

where ρ_0 and W are constants and $m = M_l/M_S$ is the ratio of local magnetization M_l to its saturation value M_S . It was

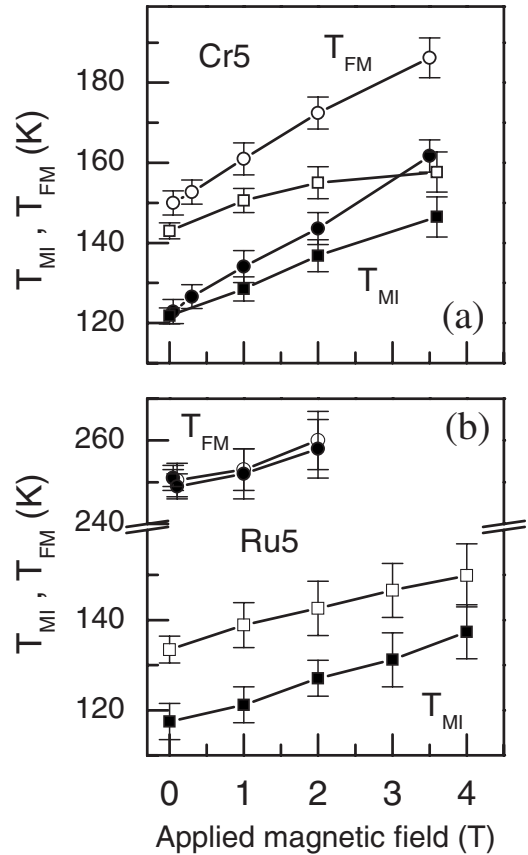


FIG. 4. Magnetic-field dependences of the metal-insulator and FM transition temperatures in the (a) Cr5 and (b) Ru5 samples. Open symbols correspond to samples with ^{16}O and closed symbols to samples with ^{18}O ; circles denote $T_{FM}(H)$ and squares denote $T_{MI}(H)$.

experimentally found out that Eq. (1) may be valid up to $m \leq 0.7$, and the negative magnetoresistance $[\rho(H)/\rho(0) - 1]$ usually exhibits quadratic field dependence in the paramagnetic state.²⁵ From the experimental point of view, it is important that magnetoresistance is a relative physical value, so that it is independent of shape and granular structure of the samples. It makes possible to study accurately the small isotope effects in m at $T > T_{FM}$, where direct absolute magnetic measurements with high resolution may be invalid. Figure 5 shows the characteristic features of isothermal magnetoresistance in manganites as an example in Ru2 samples. At high temperatures $T \geq T_{CO}$, the magnetoresistance strictly follows the quadratic law. Small but well-defined isotope shift in magnetoresistance is observed. That means that ^{16}O samples have a higher degree of ferromagnetic polarization than those with ^{18}O . As the temperature decreases, the magnetoresistance becomes subquadratic, which reflects sublinear field dependence of $M_l(H)$. In high enough magnetic field, the growth of the conductivity becomes steeper, being the precursor of field-induced metal-insulator transition. It is accompanied by the field hysteresis arising due to nucleation of FM clusters in magnetization cycle. The isotope effect in this case is more pronounced than in paramagnetic state. Based on Eq. (1), one can evaluate the local magnetic susceptibility $\chi_\sigma = M_l/H$, where M_l is calculated from the field dependence

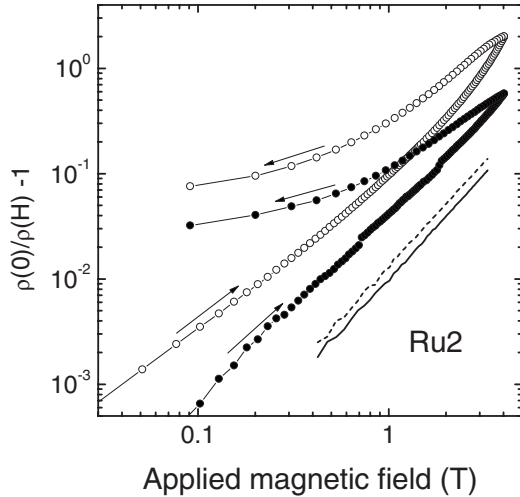


FIG. 5. Magnetoresistance $\rho(0)/\rho(H)-1$ vs applied magnetic field in Ru2 samples at $T=130$ K (open symbols correspond to samples with ^{16}O and closed symbols to samples with ^{18}O) and $T=250$ K (dashed line: ^{16}O ; solid line: ^{18}O). The arrows show the direction of the magnetization loop.

of the magnetoresistance. We assumed that $M_S=3.5\mu_B/\text{Mn}$ and $W=0.2$ eV is of the order of E_g , and both values are independent of oxygen mass and magnetic field. Figure 6 demonstrates the temperature dependence of $\chi_\sigma(T)$ in magnetic field of 1 T. $\chi_\sigma(T)$ appears to be in accordance with the small field $\chi(T)$ obtained for Cr0, Cr2, and Ru2 samples. As the FM interaction increases, the magnetic field of 1 T becomes large enough to affect the magnetization, and $\chi_\sigma(T)$ and χ may not coincide well [Fig. 6(d)]. The two major

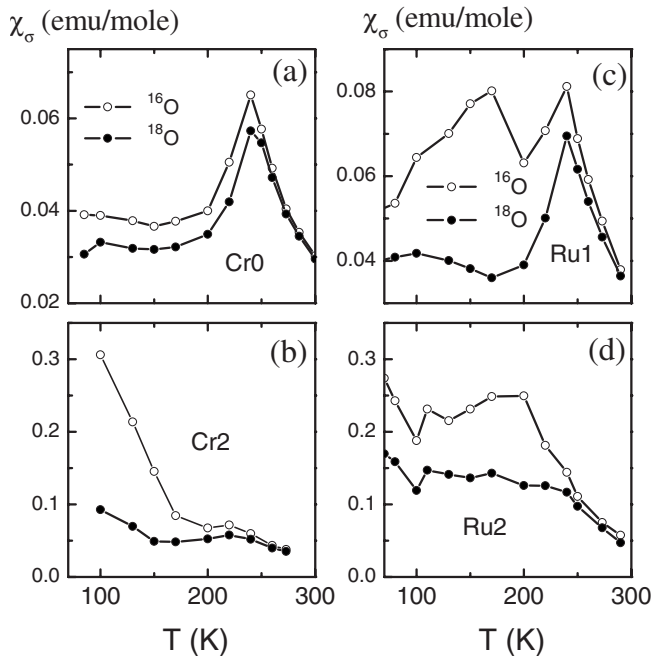


FIG. 6. Temperature dependence of susceptibility $\chi_\sigma(T)$ calculated based on magnetoresistance at $H=1.0$ T for (a) Cr0, (b) Cr2, (c) Ru1, and (d) Ru2 samples. Open symbols correspond to samples with ^{16}O and closed symbols to samples with ^{18}O .

consequences of an increase in the mass of oxygen ion in the manganite crystals are (i) the decrease in the content of the FM phase and (ii) the change in the critical temperatures T_{FM} and T_{CO} in the opposite direction: T_{FM} becomes lower, whereas T_{CO} increases.

IV. DISCUSSION

Thus, the temperature dependence of magnetic susceptibility and resistivity for $\text{Pr}_{0.5}\text{Ca}_{0.5}\text{Mn}_{1-x}\text{M}_x\text{O}_3$ manganites with $M=\text{Ru}$ and Cr at different doping levels and under the $^{16}\text{O}\rightarrow^{18}\text{O}$ isotope substitution are qualitatively similar. With increase in Cr and Ru content, the fraction of CO phase decreases alongside with the increase in the fraction of FM phase. The $^{16}\text{O}\rightarrow^{18}\text{O}$ isotope substitution leads to a shift of T_{CO} toward higher temperatures and to a decrease in T_{FM} .

However, we observed some specific features determined by the difference in interactions of Cr and Ru ions with Mn. First of all, from the results presented in Figs. 1 and 3 one sees that the effect of Cr and of Ru doping is somewhat different. Whereas even 2% of Cr is sufficient to bring about metallic conductivity for ^{16}O samples, i.e., enough to give a percolation over FM clusters, Ru2 sample is still insulating. Similarly, in the Cr5 samples there are no traces of the CO phase, whereas in Ru5 samples, one still sees some contribution of the CO phase (see Fig. 1). On the other hand, magnetism in Ru samples is at least as strong as in Cr ones (cf. the data on $\chi(T)$ for Cr and Ru in Fig. 1). One can qualitatively conclude from these data that apparently the features of FM clusters close to Cr and Ru are different: whereas Cr clusters seem to be rather big, but with weaker ferromagnetic exchange, Ru clusters are smaller, but stronger, i.e., with stronger ferromagnetic exchange and larger magnetization. In effect, e.g., in Cr5 samples, a “weak” FM phase occupies the largest part of the sample, but T_{FM} is relatively small [$T_{\text{FM}}(\text{Cr5})\approx 130$ K]. This may lead to the suppression of any traces of the long-range CO, although an appreciable difference in T_{MI} and T_{FM} in Cr5 is a signature of the important role played by the insulating phase. However, in Ru5 case, the FM clusters do not fill the whole sample (but sufficient for percolation) and some effect of the CO parts of the sample is still visible [see Figs. 1(d) and 1(f)]. But on the other hand, the stronger exchange interactions lead to a higher onset of ferromagnetism: $T_{\text{FM}}(\text{Ru5})\approx 250$ K.

In Fig. 7, we present the dependence of T_{CO} and T_{FM} on Cr and Ru doping in manganites with ^{16}O and ^{18}O . The values of the charge-ordering temperature T_{CO} coincide for samples with the same concentration of Cr and Ru. With increase in the doping level, T_{CO} decreases for the samples with Cr and Ru owing to a stronger suppression of the charge order. The $^{16}\text{O}\rightarrow^{18}\text{O}$ isotope substitution shifts T_{CO} toward higher temperatures by 4–8 K for all concentrations of Cr and Ru in the samples. In contrast, the isotope effect for the FM phase induced by impurities and magnetic field has the opposite sign. The value of T_{FM} for the samples with Ru is higher than for the samples with Cr, achieving 250 K for Ru5 sample, in agreement to the data reported in Ref. 17.

The $^{16}\text{O}\rightarrow^{18}\text{O}$ isotope substitution leads to the lowering of T_{FM} both in the samples doped by Cr and Ru well as in the

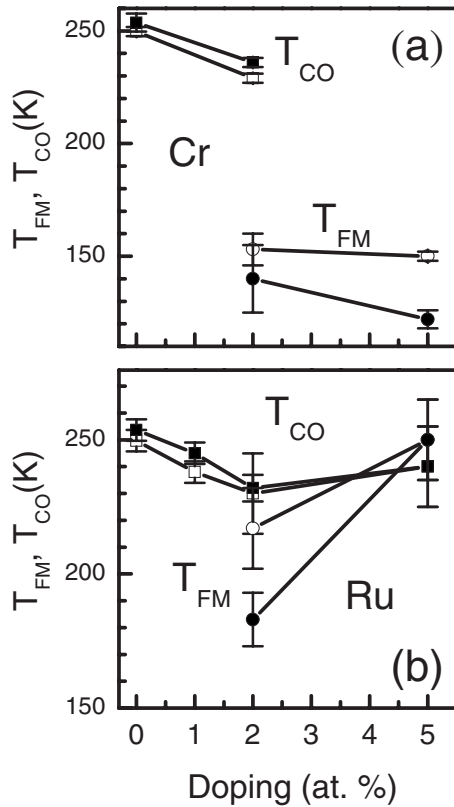


FIG. 7. Plots of the characteristic transition temperatures in the $\text{Pr}_{0.5}\text{Ca}_{0.5}\text{Mn}_{1-x}\text{M}_x^{16-18}\text{O}_3$ manganite upon (a) chromium and (b) ruthenium doping. Open symbols correspond to samples with ^{16}O and closed symbols to samples with ^{18}O . Circles denote $T_{\text{FM}}(x)$ and squares denote $T_{\text{CO}}(x)$.

other manganites. However, the value of ΔT_{FM} is not the same for different dopants. As it is shown in Figs. 1 and 2 for Cr2 and Cr5 samples, $T_{\text{FM}} \approx 130\text{--}150$ K, and its decrease is 15–25 K; ΔT_{FM} is nearly the same as for Ru2 samples with $T_{\text{FM}} \approx 180\text{--}215$ K ($\Delta T_{\text{FM}} \approx 30$ K). For Ru5 samples, T_{FM} is much higher than for the previous samples ($T_{\text{FM}} \approx 250$ K), and higher than T_{CO} , and the isotope shift ΔT_{FM} was not observed, $\Delta T_{\text{FM}} \approx 0$ K.

The most pronounced effect of the oxygen isotope substitution was observed in compounds with $x=0.02$ having minimum T_{FM} . This doping level corresponds to the region of the maximum phase separation and coexistence of phases with different order parameters. Similar results were observed in half-doped $\text{R}_{1-x}\text{Sr}_x\text{Mn}^{16-18}\text{O}_3$ manganites, where the crossover region is achieved by the heterovalent strontium doping instead of the $3d$ metal substitution of Mn (for details see the recent paper of Balagurov *et al.*²⁶ and references therein).

Using the well-known relationship $T_c \sim M^{-\alpha}$ that follows from the renormalization of the phonon frequencies, it is possible to estimate a change in the isotope exponent α related to a change in the oxygen isotope mass (M_{O}). Depending on the model accepted for the description of the isotope effect, the value of M in this relation can be represented by the isotope mass M_{O} (optical modes) or it can be the mass of the f.u. (acoustical modes). We determined α value from the experimentally measured quantities as $-\alpha \sim (\Delta T/T_c)/(\Delta M/M_{\text{O}})$.

For the FM transition, the isotope mass exponent is positive, $\alpha_{\text{FM}} = +(1.7 \pm 0.2)$ for Cr2 and Cr5 samples and $\alpha_{\text{FM}} = +(1.4 \pm 0.5)$ for Ru2 sample. According to the experimental data, the value of α_{FM} strongly decreases for Ru5 samples, $\alpha_{\text{FM}} = +(0.0 \pm 0.04)$. For the transition to a charge-ordered state, the exponent is negative and $\alpha_{\text{CO}} = -(0.15 \pm 0.02)$ for all samples with Cr and Ru. These estimates show that the isotope substitution induces a relatively small change in the temperature of transition to the charge-ordered state. In contrast, since the FM phase induced by Cr and Ru doping has the properties similar to those known for other half-doped and optimum-doped manganites, the isotope-substitution-induced change in T_{FM} is rather large and positive, with the exception for Ru5 samples.

The results presented in this paper agree qualitatively with the concepts put forward earlier^{27,28} and reveal some other aspects in the effect of oxygen isotope substitution on different phases in manganites. As to the isotope effect, it is clear that the main factor in the systems under study is the competition of two possible types of ordering, that is, charge-ordered antiferromagnetic insulator and the ferromagnetic metallic state. The increase in Cr and Ru contents, as well as the applied magnetic field, destabilize charge ordering and favor the ferromagnetic metallic state. The increase in the fraction of lighter isotope ^{16}O leads to the similar effect. On the contrary, the $^{16}\text{O} \rightarrow ^{18}\text{O}$ isotope substitution stabilizes CO state and suppresses the FM state.

An important problem, which arises in this connection, is the following: which free energy of phase, CO or FM, is more sensitive to the isotope substitution? A relative stabilization of the CO phase and destabilization of the FM phase under the $^{16}\text{O} \rightarrow ^{18}\text{O}$ isotope substitution could be related either to the lowering of the free energy F_{CO} of the CO phase (even in the absence of the long-range CO) or to the increase in the energy F_{FM} of FM phase. From the results presented above, see especially Fig. 7, one can conclude that the isotope dependence of the free energy of the CO phase plays here the main role. Indeed, for Cr-doped samples, we have $T_{\text{CO}} > T_{\text{FM}}$; that is, on cooling from high temperatures, the CO phase is the first to appear and only after that the FM phase comes into play, appearing (partially) at lower temperatures. The characteristic temperature for such a crossover, T_{FM} , is determined as that where the free energies of these competing phases become equal and the isotope effect is observed both for T_{CO} and T_{FM} . The isotope dependence of only F_{CO} is in principle sufficient for such a behavior, although the experiments only with the Cr-doped samples do not give us an opportunity to argue that F_{FM} does not depend significantly on the isotope substitution. At the same time, the situation with the Ru doping is different, and it already allows us to make such a conclusion. In fact, at small values of x we have $T_{\text{CO}} > T_{\text{FM}}$, similar to the case of Cr doping, and the isotope effect is rather strong both for T_{CO} and T_{FM} . However, at the highest doping level under study, $x=5\%$ Ru, T_{FM} exceeds T_{CO} . In this case, CO phase does not appear at all, and the system at the temperature lowering transforms directly to the FM state, i.e., T_{FM} is determined not by the competition of two phases, FM and CO, but only by the free energy of the FM phase itself. As it is illustrated in Fig. 1, the isotope effect is nearly absent for such samples, and this

supports our conjecture that the characteristics of the FM phase, in particular its free energy F_{FM} , are not strongly dependent on the isotope composition.

The observed regularity could be qualitatively explained based on the ideas discussed in Refs. 27 and 28. Charge ordering corresponds to the localization of charge carriers (electrons or holes) at certain sites of the crystal lattice. This causes the corresponding lattice distortions. A significant involvement of the crystal lattice in the charge ordering naturally leads to the dependence of its characteristics on atomic masses, i.e., on the isotope composition of the compounds under study. Although there are, in principle, different mechanisms of charge ordering, e.g., based on the intersite Coulomb repulsion of electrons, one can argue that the interaction via lattice plays an important role in manganites. It can be seen, in particular, from the fact that CO itself in $\text{Pr}_{0.5}\text{Ca}_{0.5}\text{MnO}_3$, corresponding to the checkerboard alternation of charges in the ab plane, turns out to be “in phase” in the perpendicular direction (along the c axis). A simple mechanism related to the Coulomb repulsion (Wigner crystallization) should rather favor the charge alternation in all three directions. On the other hand, the ferromagnetism in manganites is stabilized due to the double exchange mechanism in the metallic state. Itinerant electrons are less affected by the lattice and hence less sensitive to the isotope composition. The isotope effect can, of course, exist in this case too since the effective hopping integral t or the bandwidth $W = 2zt$ (z is the number of nearest-neighbor sites) could be renormalized due to the electron-phonon interaction, whereas T_{FM} is proportional to t . However, such effects are usually rather small (the dimensionless electron-phonon coupling constant does not depend explicitly on atomic mass), if the system does not correspond to the regime of small polarons.

Thus, from the experimental data presented and from the qualitative considerations, we can conclude that the isotope effect in manganites with competing CO and FM phases is predominantly caused by the dependence on the isotope composition of the free energy of the CO phase. Note, however, that the coexistence of the competing phases itself

plays here an important role. Indeed, in the absence of charge ordering, the isotope effect in T_{FM} is negligible and also the isotope effect in T_{CO} (before the onset of ferromagnetism) is not very large. The oxygen isotope substitution shifts the equilibrium between the competing phases leading to an enhancement of the isotope effect. The possible mechanisms of such an enhancement are discussed in Refs. 27 and 29.

V. CONCLUSIONS

We studied the effect of $^{16}\text{O} \rightarrow ^{18}\text{O}$ isotope substitution on the properties of $\text{Pr}_{0.5}\text{Ca}_{0.5}\text{MnO}_3$ manganite with Cr and Ru impurities. It was demonstrated that an increase in oxygen mass leads to a decrease in the concentration of the ferromagnetic metallic phase and to a significant stabilization of the charge-ordered phase. From this, one can understand several features of the behavior of these systems. Stabilization of the CO phase increases the region of its existence and leads to an increase in T_{CO} and, respectively, to a decrease in T_{FM} in case when $T_{\text{CO}} > T_{\text{FM}}$ (2% and 5% of Cr and 2% of Ru dopants). However, the isotope effect practically disappears if $T_{\text{FM}} > T_{\text{CO}}$ (5% Ru). The maximum isotope effect is observed in the region of close proximity and coexistence of phases with different order parameters. This behavior is a manifestation of a general tendency typical for manganites, namely, strong stabilization of the CO phase by $^{16}\text{O} \rightarrow ^{18}\text{O}$ isotope substitution which leads to the increase in T_{CO} and decrease in T_{FM} . As follows from our results, the dominant role here is played by the extra stabilization (decrease in the free energy) of the charge-ordered phase.

ACKNOWLEDGMENTS

The work was supported by the European project CoMePhS, Russian Foundation for Basic Research (Projects No. 07-02-00681, No. 07-02-91567-NNIOa, and No. 08-02-00212), Deutsche Forschungsgemeinschaft (Projects No. SFB 608 and No. 436 RUS 113/942/0), and the Kurchatov Institute (Initiative Project 36).

¹A. Moreo, S. Yunoki, and E. Dagotto, *Science* **283**, 2034 (1999).

²D. I. Khomskii, *Physica B* **280**, 325 (2000).

³M. Yu. Kagan, D. I. Khomskii, and A. V. Mostovoy, *Eur. Phys. J. B* **12**, 217 (1999).

⁴M. Uehara, S. Mori, C. H. Chen, and S.-W. Cheong, *Nature (London)* **399**, 560 (1999).

⁵C. I. Ventura and B. Alascio, *Phys. Rev. B* **68**, 020404(R) (2003).

⁶J. B. Goodenough, *Phys. Rev.* **100**, 564 (1955).

⁷Z. Jiráček, S. Krupička, Z. Šimša, M. Dlouha, and S. Vratilav, *J. Magn. Mater.* **53**, 153 (1985).

⁸R. Kajimoto, T. Kakeshita, Y. Oohara, H. Yoshizawa, Y. Tomioka, and Y. Tokura, *Phys. Rev. B* **58**, R11837 (1998).

⁹M. v. Zimmermann, J. P. Hill, D. Gibbs, M. Blume, D. Casa, B. Keimer, Y. Murakami, Y. Tomioka, and Y. Tokura, *Phys. Rev. Lett.* **83**, 4872 (1999).

¹⁰M. Tokunaga, N. Miura, Y. Tomioka, and Y. Tokura, *Phys. Rev. B* **57**, 5259 (1998).

¹¹B. Raveau, A. Maignan, and C. Martin, *J. Solid State Chem.* **130**, 162 (1997).

¹²A. Maignan, F. Damay, C. Martin, and B. Raveau, *Mater. Res. Bull.* **32**, 965 (1997).

¹³A. Barnabe, A. Maignan, M. Hervieu, F. Damay, C. Martin, and B. Raveau, *Appl. Phys. Lett.* **71**, 3907 (1997).

¹⁴P. V. Vanitha, A. A. Arulraj, A. R. Raju, and C. N. R. Rao, *C.R. Acad. Sci., Ser. II: Chim* **2**, 595 (1999).

¹⁵B. Raveau, M. Hervieu, A. Maignan, and C. Martin, *J. Mater. Chem.* **11**, 29 (2001).

¹⁶S. Hébert, A. Maignan, C. Martin, and B. Raveau, *Solid State Commun.* **121**, 229 (2002).

¹⁷C. Martin, A. Maignan, M. Hervieu, C. Autret, B. Raveau, and D. I. Khomskii, *Phys. Rev. B* **63**, 174402 (2001).

- ¹⁸A. Maignan, C. Martin, S. Hébert, and B. Raveau, *J. Appl. Phys.* **89**, 500 (2001).
- ¹⁹N. A. Babushkina, L. M. Belova, O. Yu. Gorbenko, A. R. Kaul, A. A. Bosak, V. I. Ozhogin, and K. I. Kugel, *Nature (London)* **391**, 6663 (1998).
- ²⁰N. A. Babushkina, E. A. Chistotina, O. Yu. Gorbenko, A. R. Kaul, D. I. Khomskii, and K. I. Kugel, *Phys. Rev. B* **67**, 100410(R) (2003).
- ²¹N. A. Babushkina, A. Maignan, A. N. Taldenkov, A. V. Inyushkin, and E. A. Chistotina, *Zh. Eksp. Teor. Fiz.* **132**, 129 (2007) [*JETP* **105**, 112 (2007)].
- ²²T. Nishioka and N. K. Sato, *J. Magn. Magn. Mater.* **272-276**, 2305 (2004).
- ²³Z. Jirák, F. Damay, M. Hervieu, C. Martin, B. Raveau, G. André, and F. Bourée, *Phys. Rev. B* **61**, 1181 (2000).
- ²⁴J. P. Franck, I. Isaac, G. Zhang, J. E. Gordon, C. Marcenat, R. Lortz, C. Meingast, F. Bouquet, R. A. Fisher, and N. E. Phillips, *J. Supercond.* **15**, 571 (2002).
- ²⁵M. Tokunaga, N. Miura, Y. Moritomo, and Y. Tokura, *Phys. Rev. B* **59**, 11151 (1999); N. G. Bebenin and V. V. Ustinov, *J. Phys.: Condens. Matter* **10**, 6301 (1998); P. Wagner, I. Gordon, L. Trappeniers, J. Vanacken, F. Herlach, V. V. Moshchalkov, and Y. Bruynseraede, *Phys. Rev. Lett.* **81**, 3980 (1998); G. Jakob, W. Westerburg, F. Martin, and H. Adrian, *Phys. Rev. B* **58**, 14966 (1998).
- ²⁶A. M. Balagurov, I. A. Bobrikov, V. Yu. Pomjakushin, D. V. Sheptyakov, N. A. Babushkina, O. Yu. Gorbenko, M. S. Kartavtseva, and A. R. Kaul, *Zh. Eksp. Teor. Fiz.* **133**, 605 (2008) [*JETP* **106**, 528 (2008)].
- ²⁷N. A. Babushkina, L. M. Belova, V. I. Ozhogin, O. Yu. Gorbenko, A. R. Kaul, A. A. Bosak, D. I. Khomskii, and K. I. Kugel, *J. Appl. Phys.* **83**, 7369 (1998).
- ²⁸N. A. Babushkina, L. M. Belova, A. N. Taldenkov, E. A. Chistotina, D. I. Khomskii, K. I. Kugel, O. Yu. Gorbenko, and A. R. Kaul, *J. Phys.: Condens. Matter* **11**, 5865 (1999).
- ²⁹N. M. Plakida, *Pis'ma Zh. Eksp. Teor. Fiz.* **71**, 720 (2000) [*JETP Lett.* **71**, 493 (2000)].